SIMULATION OF SLIDE-COATING FLOWS USING A FIXED GRID
AND A VOLUME-OF-FLUID FRONT-TRACKING TECHNIQUE
Startup and Bead Breakup*†

C.W. Hirt
Flow Science, Inc.
1325 Trinity Dr.
Los Alamos, NM 87544

Ken S. Chen
Engineering Sciences Center
Sandia National Laboratories
Albuquerque, NM 87185-0826

ABSTRACT

Slide coating flow is a workhorse process for manufacturing precision film-coating products. Properly starting up a slide coating process is very important in reducing wastage during startup and ensuring that the process operates within the desired 'coating window.' A two-phase flow analysis of slide-coating startup was performed by Palmquist and Scriven (1994) using Galerkin's method with finite-element basis functions and an elliptic mesh generation scheme. As reported by Chen (1992) from flow visualization experiments, a continuously coated liquid film breaks up into rivulets, which are coating stripes with dry lanes in between, when the coated film becomes thinner and thinner due to either the increase in substrate speed or the reduction in pre-metered feed-liquid pump speed. It was observed that the coated-film breakup process originated from the coating bead, thus the name of bead breakup. Understanding the bead-breakup phenomena and elucidating mechanisms involved will provide guidance for manufacturing thinner coating, an industrial trend for better product performance.

In this paper we present simulation results of slide-coating flows obtained from a computational method capable of describing arbitrary, three-dimensional and time-dependent deformations. The method, which is available in a commercial code, uses a fixed grid through which fluid interfaces are tracked by a Volume-of-Fluid technique (Hirt and Nichols, 1981). Surface tension, wall adhesion, and viscous stresses are fully accounted for in our analysis. We illustrate our computational approach by application to startup and the bead-breakup problems. As will be shown, for rapid processes our approach offers the computational efficiency and robustness that are difficult to achieve in conventional finite-element-based methods.

DISCLAIMER

Portions of this document may be illegible in electronic image products. Images are produced from the best available original document.

I. INTRODUCTION

Slide coating flow is a workhorse process for manufacturing precision film-coated products. Properly starting up a slide coating process is very important in reducing waste during startup and ensuring that the process operates within the desired coating window. The startup process involves a complex flow in which the coating material can undergo large deformations before achieving steady coating conditions.

The same can be said for the bead breakup process. In both cases, the coating liquid is subject to strong surface tension forces, viscous stresses, and fluid/solid adhesion forces. To a lesser extent the coating is also subject to gravitational body forces and to applied vacuum pressures used to control the coating bead.

The dynamics of flow in a coating bead are strongly non-linear, making it difficult to analyze with purely analytical tools. Experimental studies, on the other hand, are hampered by the small size and the multitude of parameters that characterize the slide-coating process. These conditions suggest the use of advanced computational models.

In this paper we have applied a commercial computational fluid dynamics program, FLOW-3D®, developed by Flow Science, Inc. to several slide-coating problems. Our examples focus on transient phenomena associated with startup and breakup processes because these are traditionally the hardest problems to simulate. Not only are these problems difficult because of their time dependence, they often involve large deformations, breakup, and coalescence of the coating liquid.

The advantage of the modeling tool we have chosen is that it uses a robust numerical technique, the Volume-of-Fluid (VOF) method, which has the power to track arbitrary fluid interfaces. A brief description of this method, and other features of the FLOW-3D program crucial to our analysis, are given in the next section. The problem we have chosen to study is described in Section III. In Section IV we present a series of two-dimensional studies of transient bead phenomena. In Section V are the results of a three-dimensional simulation of bead breakdown into rivulets. Finally, Section VI summarizes the approach and results obtained with this new coating simulation tool.

II. OVERVIEW OF NUMERICAL METHOD

There are many numerical approaches used to solve the equations of mass, momentum, and energy conservation describing a fluid. Our interest here is in incompressible, isothermal liquids having free boundaries (i.e., surfaces in contact with air or some other gas). The liquid must have inertia and respond to internal and surface (gas) pressures, viscous stresses, surface tension, and gravitational forces. A powerful and popular method developed to treat such problems originated at the Los Alamos National Laboratory in the mid 1960s under the name Marker-and-Cell (MAC) method (Harlow and Welch, 1965). Many variations and improvements in the basic MAC technique have been reported in the literature over the years (see, e.g., Roach, 1972).

One improvement to the original MAC approach has been in the way free boundaries are modeled using the VOF method. The basis of this method is a fixed grid of rectangular control volumes. For each control volume a number, F, is kept to denote the fraction of the volume that is occupied by liquid. Thus, an F=1 value indicates a control volume completely filled with liquid, while an F=0 value indicates a volume with no liquid. Control volumes only partially filled, 0<F<1, contain the liquid surface.

Liquid is computed to move through the grid and/or deform by suitably changing the F values for each grid volume. Since the grid doesn't move, and because we only record the fractional volume of each cell occupied by liquid, we have no difficulty in representing the breakup or coalescence of liquid regions. The key to this method is that liquid surfaces are easily reconstructed from the F values after they have been changed. Furthermore, it is possible to compute surface areas, surface normals, and surface curvatures from the F values (see e.g., Hirt and Nichols, 1981). These are the quantities needed for the application of boundary conditions and the evaluation of surface tension and wall adhesion forces.

The complete solution method consists of a MAC-like solver in those grid cells completely occupied by liquid. Cells containing liquid surfaces are set to supply appropriate boundary conditions.

A time-dependent solution is computed in a series of small time steps. After each time step, liquid surfaces are moved by updating the F function, which is governed by a special advective transport equation that maintains sharp interfaces. Then the solution process is repeated for another time step, over and over again, until the complete time interval of the simulation has been covered.

We shall not give details of the difference equations, numerical stability conditions, or other considerations that make up a complete solution algorithm because they have been amply reported elsewhere (see, e.g., Roach, 1972). We shall, however, briefly discuss a couple of important differences between the present numerical method and conventional finite-element methods.

There is no complicated grid generation in our method, which uses a simple rectangular array of control volumes. This greatly simplifies the numerical method and requires less computer memory; but it also means that we cannot deform the grid, e.g., to conform to the geometry of a slide coater. Instead, we represent complex geometry using a technique referred to as the Fractional-Area-Volume-Obstacle Representation (FAVOR) method (Hirt & Sicilian, 1985; Hirt, 1992).

In the FAVOR method, obstacles are embedded in the fixed grid by allowing them to block portions of grid cell faces and cell volumes. When these area/volume blockages are accounted for in the finite-volume equations, the geometry is automatically taken into account. FAVOR is a robust way to preserve the simplicity of the numerical scheme while representing complex geometric regions.

Another useful feature of the control volume approach is that contact lines (i.e., lines where coating liquid, air, and solid surfaces meet) require no special treatment. All forces and convective

fluxes affecting liquid in volume elements containing contact lines are averaged over the control volume. The contact line simply moves as the liquid evolves according to the F (fluid fraction) values. The computed contact angle is dynamic because it is the outcome of the local balance of forces.

Of course, accuracy improves as the control volume size is reduced. It isn't necessary, however, to use exceptionally small volumes, only volumes small enough to resolve the variations in mean flow properties.

Finally, we note that FLOW-3D has been extensively validated against a wide range of data, including many examples involving strong surface tension and viscous forces.

III. SLIDE COATING MODEL PROBLEM

The slide coating problem used as the basis for the simulations reported in this paper was taken from the thesis work of one of the authors (Chen, 1992) in which various coating defects were investigated experimentally. The coating liquid was a glycerine-water solution that behaves as a Newtonian fluid. The properties of this liquid are: density of 1000 Kg/m^3, viscosity of μ=0.0124 Kg/m/s, surface tension of σ=0.066 Kg/s^2 and static contact angle of 30 degrees.

For the exploratory calculations presented here, we used a somewhat smaller surface tension of σ=0.01 Kg/s^2, to reduced computational times. This change increased the capillary number of the flow, but it was still well below the range investigated in the experiments.

The problem, see Fig. 1, consists of a web surface to be coated, which is at the left side oriented vertically and moving upward at a speed of 0.2 to 0.3 m/s. To the right of the web there is a slide plate tilted upward 30 degrees with respect to the horizontal (dark shaded region in Fig. 1). The distance between the tip of the slide and the web is nominally 250 μm, although this distance varies in some of our examples.

Coating liquid is introduced at the right side of the computational grid with a thickness of 649 μm and a speed tangent to the slide surface of 0.0277 m/s. This speed was selected as the average speed the coating liquid would achieve in steady flow down the slide surface under the action of gravity alone. The flow rate per unit width of slide was 1.8e-5 m^2/s.

For a web speed of U=0.2 m/s the capillary number of the flow, $\mu U/\sigma$, was 0.248, and mass conservation requires the web coating thickness to be 90μm when steady conditions are reached.

In Fig. 1, we have overlaid a typical computational grid and shown the computed velocity vectors from a preliminary calculation, which graphically depicts how liquid interfaces and obstacles are defined within the grid of fixed control volumes.

The grid in most cases consisted of a non-uniform arrangement of 25 cells in the x direction and 40 cells in the z direction. Only one cell was used in the y direction for two-dimensional studies

4

but was increased to 40 cells covering a length of 4000µm for the three-dimensional cases (a total of 40,000 control volumes).

No vacuum pressure was used below the slide lip for any of the simulations, although this is a capability of the modeling program that could be used in future studies.

The experimental results obtained with this arrangement indicated stable, uniform coating at web speeds at least up to 0.191 m/s. First bead breakup was observed at a web speed of 0.237 m/s. We shall use the borderline value of 0.2 m/s for our steady-state studies and 0.3 m/s to study the breakup process.

IV. TWO-DIMENSIONAL TRANSIENT PHENOMENA

Drip Off

We begin by computing the gap between the web and slide necessary such that no coating of the web will occur. This distance is the maximum width reached by the liquid as it flows down the side and drips off the end. The maximum distance is greater than the steady-state runoff case because the eventual wetting of the bottom of the slide helps to pull liquid around the slide edge.

Computed results for the drip off are shown in Fig.2. The maximum drip thickness, about 1016 µm, occurs in the middle frame when the inertia of the liquid flowing off the top of slide is just beginning to be strongly influenced by the attachment of liquid on the bottom of the slide. By the time of the last frame, there is sufficient liquid below the lip of the slide that gravity is causing a large downward velocity pulling the liquid around the slide edge. At this time the width of the drip has been reduced to 955 µm.

Steady Coating - No Under-Lip Wetting

Setting the web-to-lip gap at 250 µm, we computed the flow evolution for a period of 0.3 s, starting from the same initial condition used for the previous example. Snapshots of the transient as a steady-state flow condition is established are shown in Fig. 3A. At early times (frame 2) the bead is quite thick, and there is some recirculation in the bead. As time progresses, both the bead and the coating on the web monotonically become thinner. Steady conditions (last frame) are reached by about 0.2 s.

Although the static contact angle was specified as 30 degrees, the angle between the coating material and the slide surface is closer to 70 degrees, see closeup in Fig.3B. This is an example where pressure forces and the viscous entrainment of liquid away from the contact point are competing with adhesion forces to produced a "dynamic" contact angle.

This computation required about 5 CPU hours to reach steady state on an older workstation, an IBM RS6000/320. On a 133MH Pentium PC computer the time would be about 1.0 hour!

It is useful to note that no coating liquid is under the lip of the slide. This leads to a tenuous force balance in which the flow may be disturbed by moving the contact point on the slide surface.

Steady Coating - With Under-lip Wetting

If we initialize the liquid with a small amount of liquid extending under the lip of the slide, steady conditions are reached in about half the time compared with the previous case, and the bead is thicker than in the previous case. Fig. 4 shows the modified initial condition and the resulting steady-state flow, which contains a small recirculation region at the top of the bead. Here the contact point on the slide is closely tied to the slide lip and is less easily moved to other positions.

Effect of an Increasing Gap

Coating beads are highly sensitive to the gap between the lip of the slide and the web because this distance has a direct effect on the curvatures (i.e., surface tension forces) along the top and bottom sides of the bead. With this in mind it is interesting to see what happens when the gap is slowly increased.

Beginning with the previous steady-state condition (with under-lip wetting and a web speed of 0.2 m/s), we allowed the gap to open at a steady 500 μm/s. At this rate it takes 0.5 seconds to double the initial gap width.

Snapshots of the transient are shown in Fig. 5. As the gap begins to open, there is an immediate response observed at the contact point on the web (t=0.105). Opening the gap immediately alters the dynamic balance at the contact point, and it quickly moves upward approximately 300 μm causing both a thinning of the bead and a thinning of the coating on the web.

The contact point motion is temporarily arrested by surface tension forces just before there is a complete breakdown of the bead (t=0.115). For a short time the bead thickens (t=0.125) but then thins again as the gap continues to increase (t=0.16). Finally, the bead breaks and liquid remaining on the slide rapidly retracts because of surface tension (t=0.20).

The oscillations in bead thickness in this example clearly show a competition between forces acting on the coating bead. It is also clear that the stability of the bead is closely regulated by surface tension forces acting along the underside of the bead.

Effect of a Sudden Gap Decrease

Sudden gap changes can occur when splices in the web travel by the lip of the slide. A simple example of this type of transient can be arranged in our calculational method by allowing a thin obstacle to be attached to the web. By way of illustration we used an obstacle 60 μm in thickness to perturb the flow in the case with under-lip wetting.

The consequences of a sudden decrease in gap thickness by 24% are shown in Fig.6. In the first frame the obstacle has just pushed into the coating liquid at the bottom of the bead. A short time later (frame two) the bead has thickened while the coating thickness on the obstacle has been greatly reduced.

At first sight it seems odd that the coating thickness would be reduced since the gap has been reduced and the obstacle is moving at the same speed as the original web to which it is attached. The reason, however, is easily explained by closer examination of the flow in the bead. The smaller gap has increased the influence of surface tension on the underside of the bead causing a net flow of material into that region. This flow is apparently strong enough to overcome the upward viscous stresses exerted on the liquid by the obstacle.

The reduced coating thickness does not last for long because the underside of the bead quickly stabilizes (third frame), and the web-obstacle begins to carry off liquid once again.

This is a good example of the type of complex, and unanticipated, transient phenomena that can be revealed by computational modeling.

Effect of a Web Speed Change

Experiments indicate bead breakup should occur if the web speed is increased above 0.237 m/s. Breakup, however, always begins near an end wall of the slide where there are strong three-dimensional curvatures in the liquid surfaces. As a preliminary to three-dimensional simulations, we now ask what happens to the two-dimensional bead when the web speed is suddenly increased from 0.2 m/s to 0.3 m/s in a time interval of 0.001 seconds? The final value of 0.3 m/s has been selected to be above the experimentally observed breakup speed.

Figure 7 shows the transient that develops in the case when the bottom side of the slide was wetted. Beginning from steady conditions at t=0.1 s, the bead immediately thins as the liquid contact point on the web is carried upward. Coating liquid is carried off by the web as a temporarily thicker coating, see t=0.11 s results in Fig.7.

By t=0.14 s the coating on the web is much thinner, and the contact point of the liquid on the web has moved further upward. The flow has more or less stabilized by t=0.2 s, last frame in Fig.7. At this time, pressures across the bead are nearly uniform, and the contact point is nearly stationary.

An important result of this calculation is that the bead remains intact at a web speed of 0.3 m/s. This supports observations that rivulet formation begins at an end wall of the slide where there are three-dimensional curvatures and not because of a general breakdown in the coating process.

V. THREE-DIMENSIONAL TRANSIENT PHENOMENA

The goal of most coating processes is to produce a near perfect two-dimensional surface. Unfortunately, three-dimensional effects cannot be avoided. Some three-dimensional effects arise spontaneously because of flow instabilities, but these can be minimized by carefully controlling the coating process. Other three-dimensional effects are introduced by the coating system itself, for example, at the sides of the coating slide where some three-dimensional structure must form because of the discontinuities existing there.

In the next two sections we take a preliminary look at both these types of three-dimensional phenomena.

Three-Dimensional Startup Flow

To investigate edge conditions during startup, we model a section of the slide 4000 μm long (i.e., 16 times the gap thickness). At one end there is a rigid, stationary wall attached to the slide. At the other end of this section we use symmetry conditions. Initial conditions are identical to those used for the two-dimensional examples without under-lip wetting. That is, the web speed was 0.2 m/s and some coating liquid existed on the top of the slide at the beginning of the simulation but did not span the gap and contact the web (see first frame of Fig.3A).

Results of this simulation are presented in Fig.8. By t=4 ms, wall adhesion is pulling liquid up the end wall sending a capillary depression wave moving along the lip of the slide away from the wall. Shortly afterwards, coating liquid on the end wall reaches the web. It is interesting to note that liquid away from the end wall does not began to coat the web uniformly because of the capillary wave. A delay occurs in the region of wave depression, while immediately ahead of the wave there is a slight bulge accelerating the time of coating, see t=16 ms.

After 26 ms liquid along the entire length of the slide has reached the web but is not yet coating it uniformly. Uniform conditions are nearly established by t=40 ms, although a small capillary wave still exists close to the symmetry end of the slide. This wave does not seem to be influencing the uniformity of the coating leaving the top of the computational region.

We note that the coating thickness is about twice as large in a small region near the end wall. Furthermore, it is easy to see there are strong three-dimensional curvatures in the region of the stationary end wall as would be expected.

Three-Dimensional Rivulet Initiation

Using the previous calculation as a starting point, we instantaneously increased the web speed from 0.2 m/s to 0.3 m/s. After a few milliseconds of simulation time, a tear opens in the coating in the transition region between the end-wall flow and flow over the remainder of the slide, Fig.9. Presumably the increase in web speed tries to pull more liquid away from the slide, but slower moving liquid near the end wall is unable to respond as quickly as elsewhere.

8

This tear continues to open up, primarily because of surface tension forces that are contracting the surfaces along the gap in an attempt to reduce the surface area. This produces wet and dry regions (rivulets) on the web with vertical edges.

In this case, it is likely that the ultimate rivulet size is controlled by the limited extent of the simulation and by the assumption of symmetry at the end of the slide opposite the end wall. Nevertheless, the occurrence of breakdown at the transition region between the end-wall conditions and the remainder of the slide should be realistic because this region was adequately resolved.

VI. DISCUSSION

We have computationally analyzed startup and bead-breakup phenomena associated with the slide-coating process. Our results were obtained with a numerical method that tracks fluid interfaces through a grid of fixed control volumes. The results presented are not meant to be exhaustive but rather to illustrate the power of this computational tool for application to many difficult coating flow problems.

Our goal has been to show that it is possible to numerically study coating flows involving transient phenomena that cannot easily be studied by more traditional computational methods. The fact that our analysis has been performed by the commercially available product, FLOW-3D, shows that analysis tools are now available for understanding many complex phenomena involved in slide coating.

REFERENCES

Chen, K. S., 1992, "Studies of Multilayer Slide Coating and Related Processes," Ph.D. Thesis, University of Minnesota, Minneapolis.

Harlow, F.H. and Welch, E., 1965, "Numerical Calculation of Time-Dependent Viscous Incompressible Flow of Fluid with Free Surfaces," Phys. Fluids, 8, 2182.

Hirt, C.W. and Nichols, B.D., 1981, "Volume of Fluid (VOF) Method for the Dynamics of Free Boundaries," JCP 39, 201.

Hirt, C.W. and Sicilian, J.M., 1985, "A Porosity Technique for the Definition of Obstacles in Rectangular Cell Meshes," Fourth Int'l. Conf. Ship Hydrodynamics, Washington, DC, September 1985.

Hirt, C.W., 1992, "Volume-Fraction Techniques: Powerful Tools for Flow Modeling," Proc. Comp. Wind Eng., University of Tokyo, August 1992.

Palmquist, K.E. and Scriven, L.E., 1994, "Start-up of Slide Coating:Steady-State Models," presented at the 1994 Int'l. Coating Process Science & Technology Symp., paper 2a, AIChE Spring Nat. Mtg., Atlanta, GA, April 17-21.

Roach, P.J., 1972, Computational Fluid Dynamics, Hermosa Publishers, Albuquerque, NM.
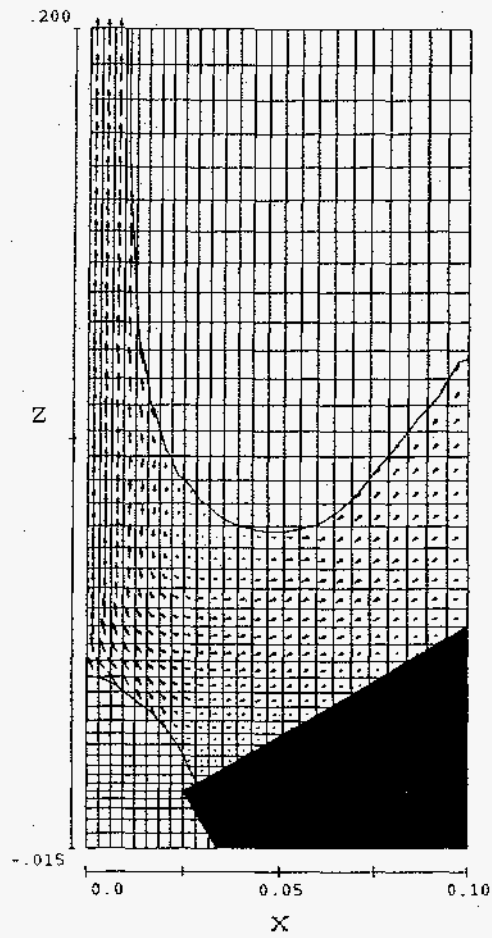
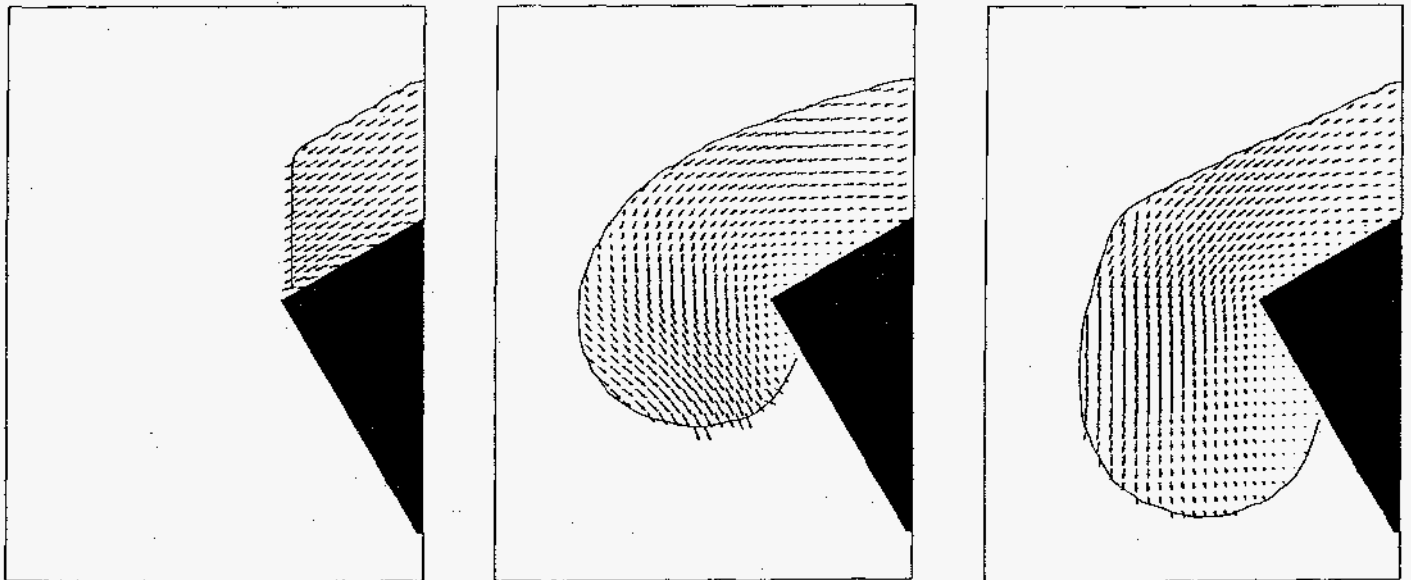Fig. 1. Grid overlaid on bead region of a slide coater.

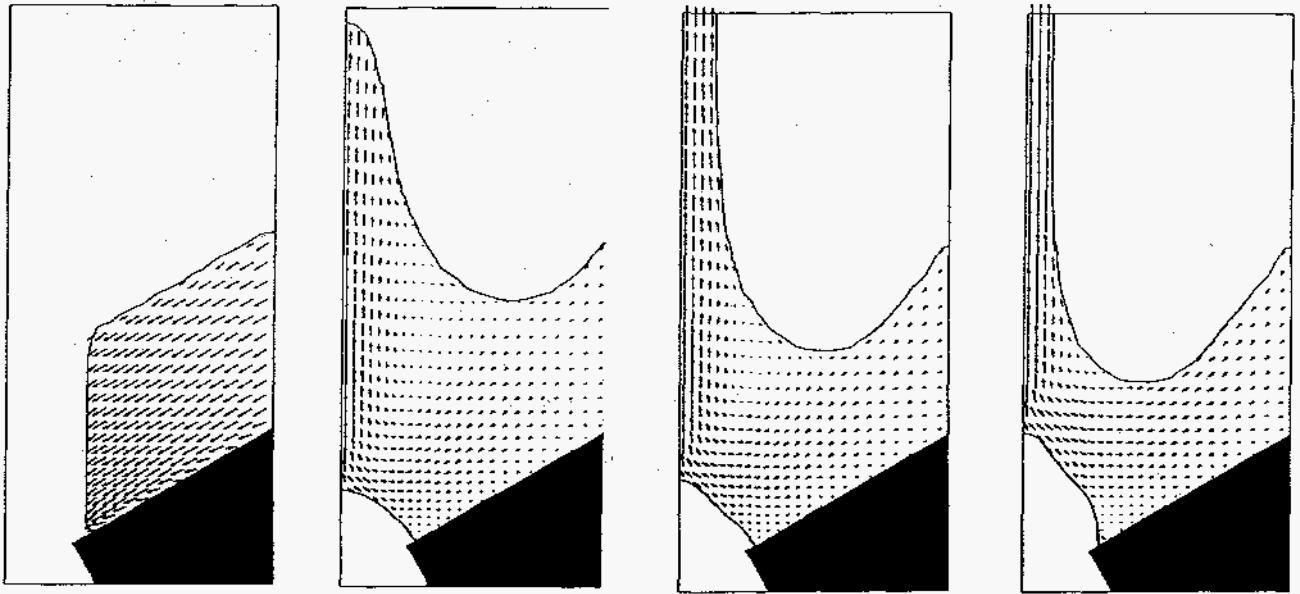Fig. 2. Drip off transient. Times are 0.0, 0.08 and 0.1 s.

Fig. 3A. Establishing a steady flow condition. Times are 0.0, 0.025, 0.05 and 0.3 s.
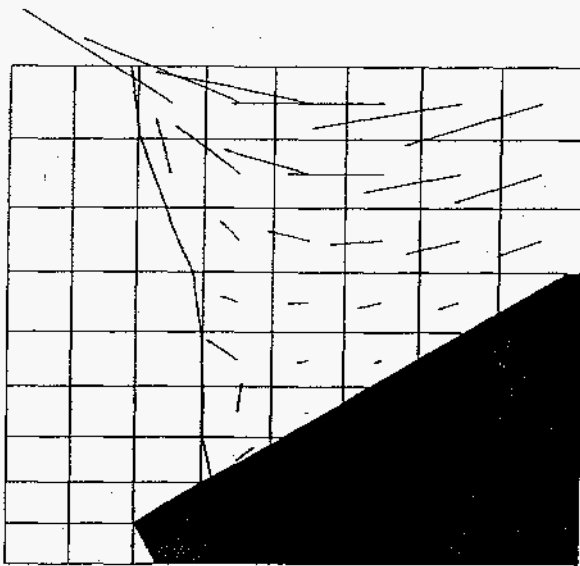

Fig. 3B. Closeup of contact point
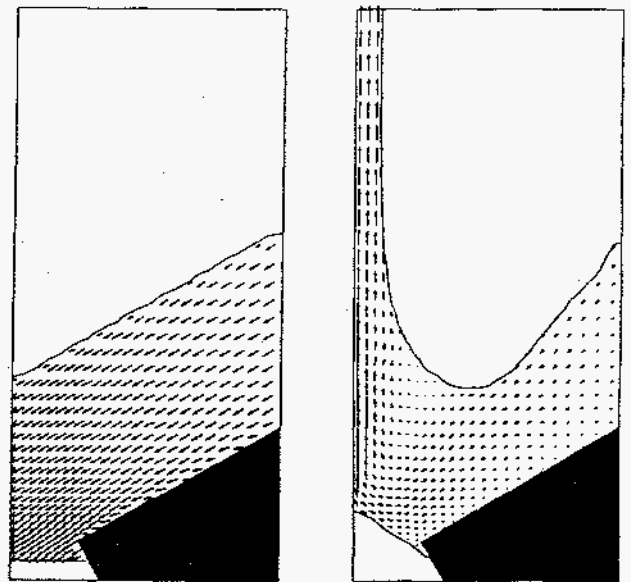on slide (shaded region).

Fig. 4. Initial and steady-state result
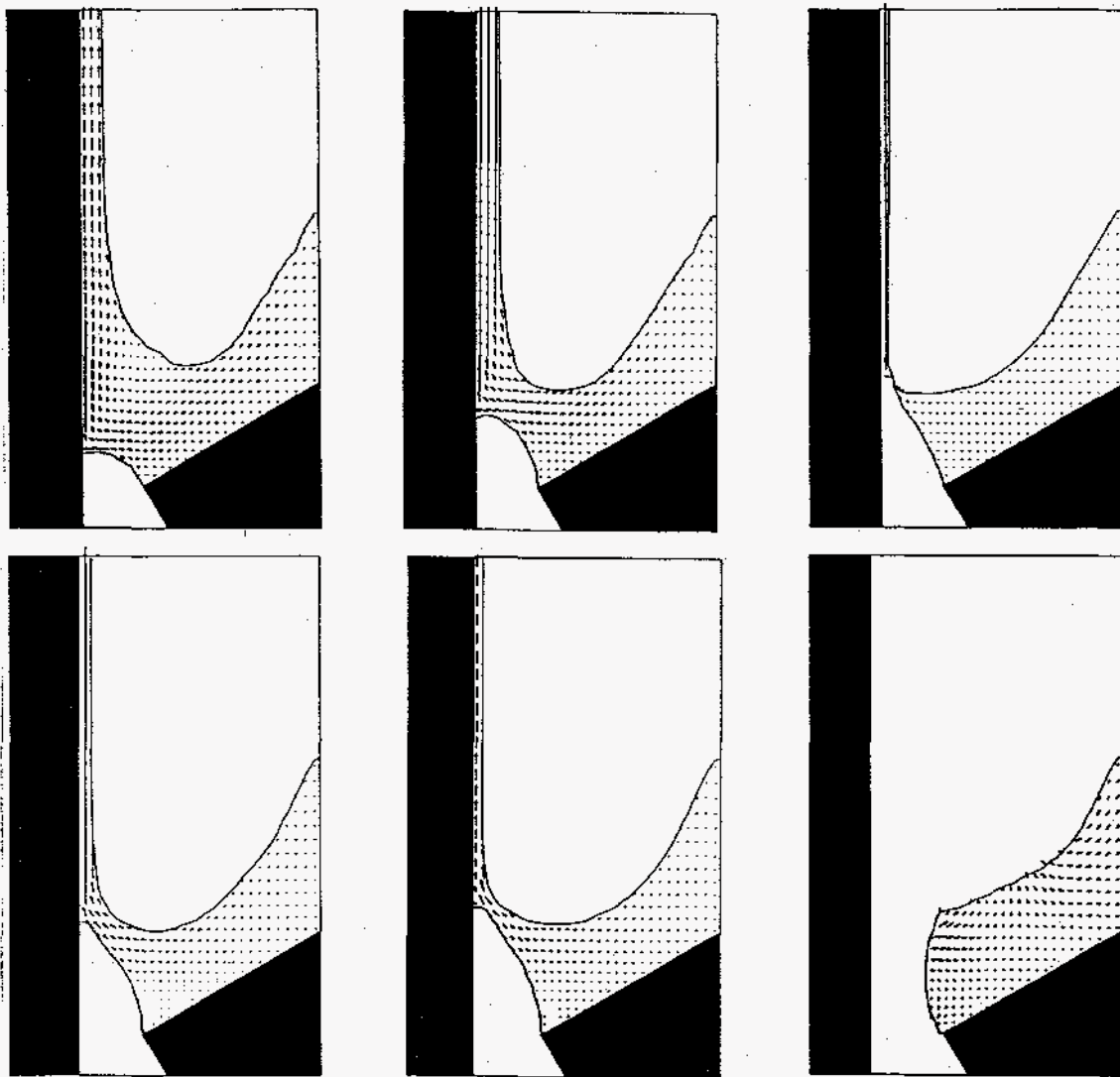or under-lip wetting.

Fig. 5. Results of moving web to left. Times are 0.095, 0.105, 0.115, 0.125, 0.16 and 0.2 s.
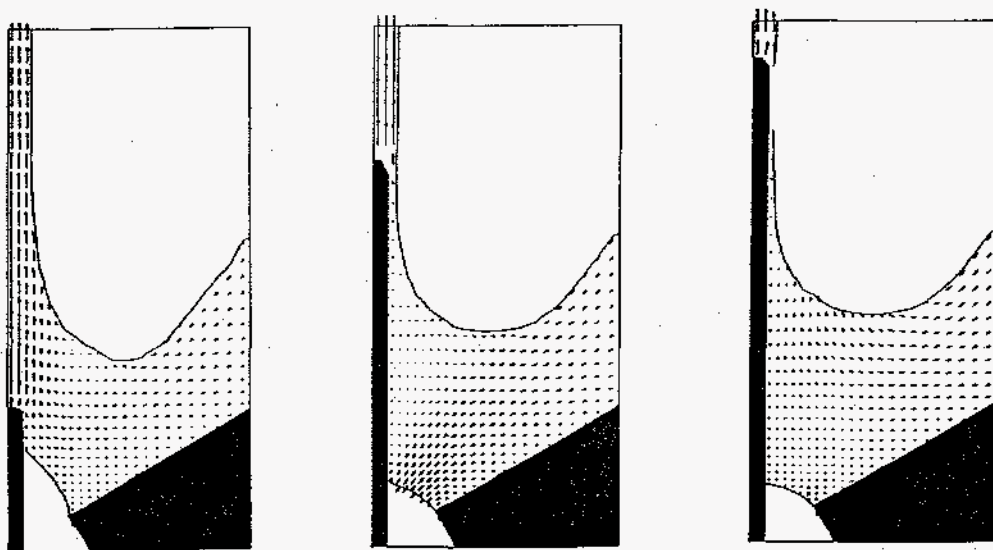

Fig. 6. Results of reducing gap with splice on web. Times are 0.103, 0.108 and 0.11 s.
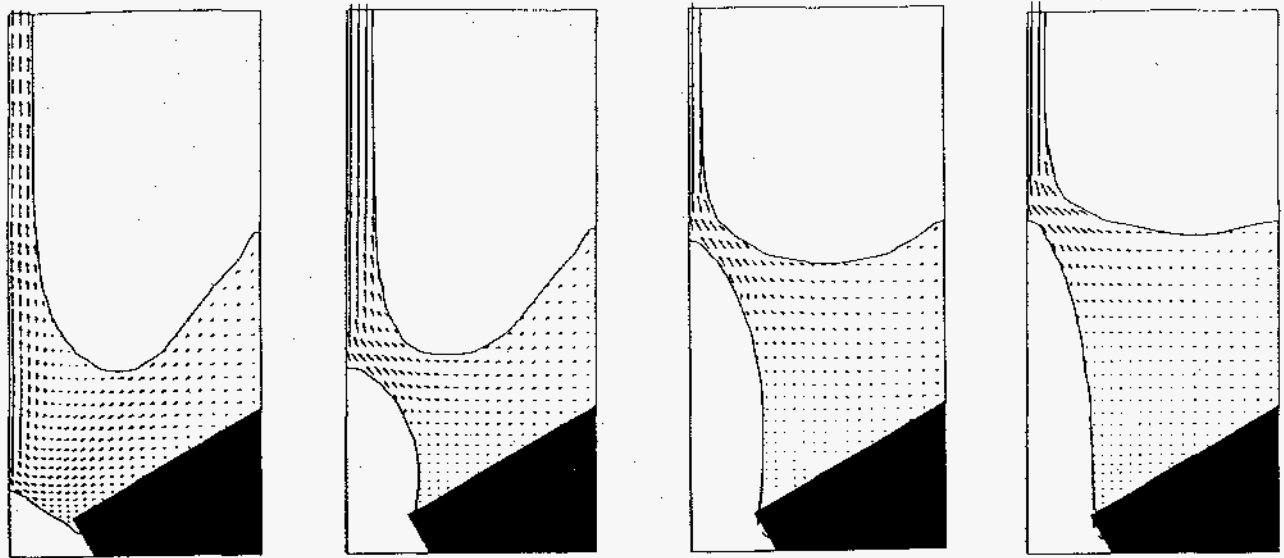
Fig. 7. Results of increasing web speed from 0.2 to 0.3 m/s. Times are 0.1, 0.11, 0.14 and 0.2 s.
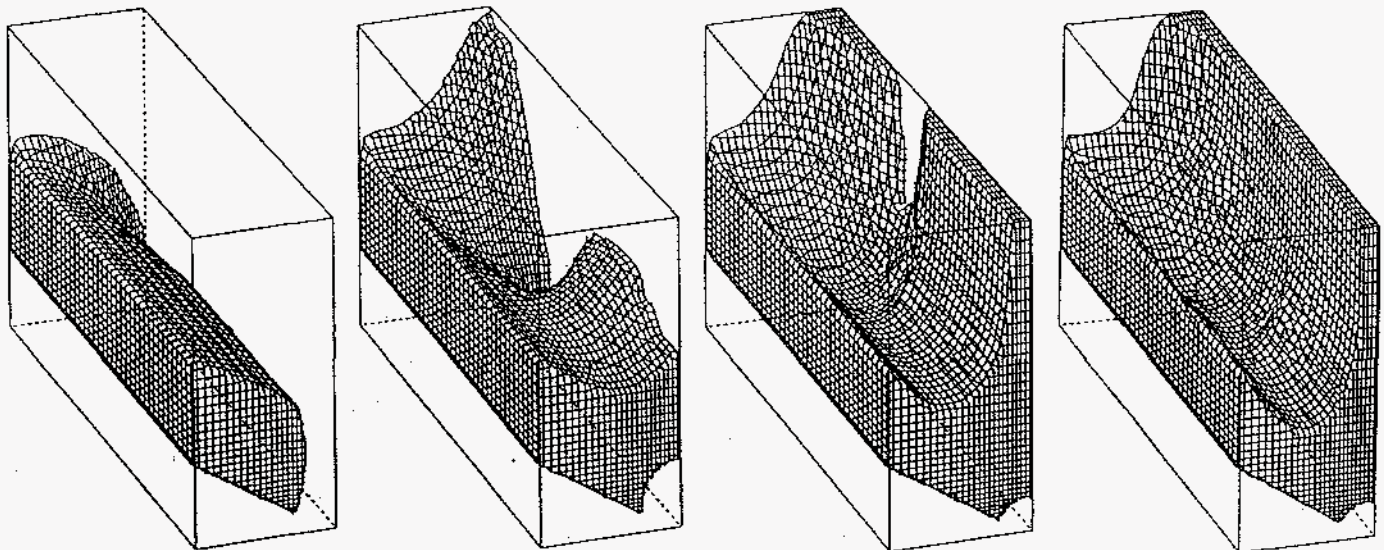
Fig. 8. Startup transient near end plate. Times are 0.004, 0.016, 0.026 and 0.04 s.
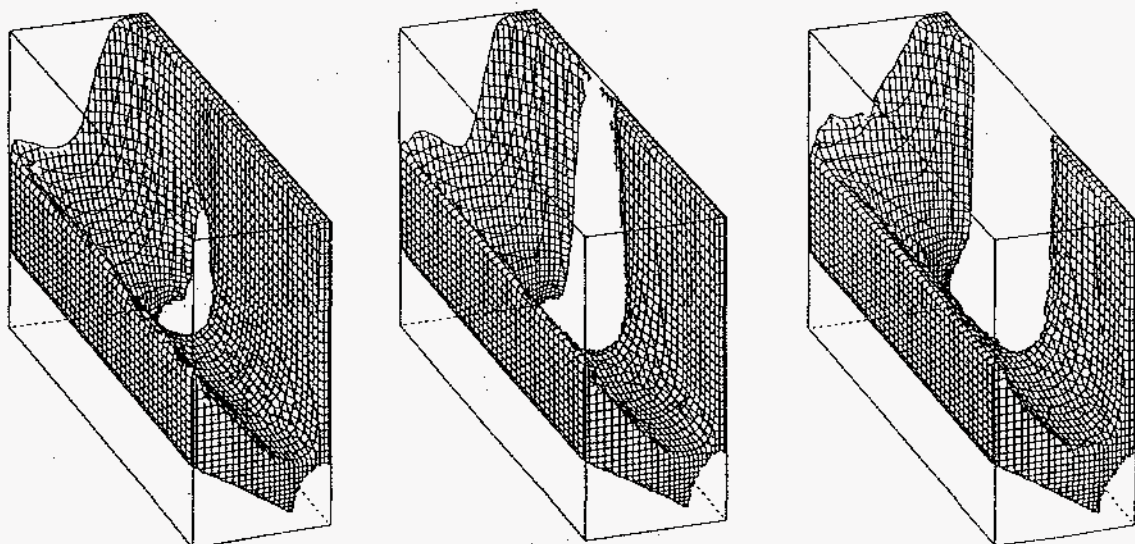
Fig. 9. Rivulet formation when web speed is increased. Times are 0.0562, 0.065 and 0.0833 s.

DISCLAIMER